The American Journal of Human Genetics, Volume *101*

Supplemental Data

Allelic Expression Imbalance Promoting a Mutant *PEX6* Allele Causes Zellweger Spectrum Disorder

Kim D. Falkenberg, Nancy E. Braverman, Ann B. Moser, Steven J. Steinberg, Femke C.C. Klouwer, Agatha Schlüter, Montserrat Ruiz, Aurora Pujol, Martin Engvall, Karin Naess, FrancJan van Spronsen, Irene Körver-Keularts, M. Estela Rubio-Gozalbo, Sacha Ferdinandusse, Ronald J.A. Wanders, and Hans R. Waterham

Supplemental data

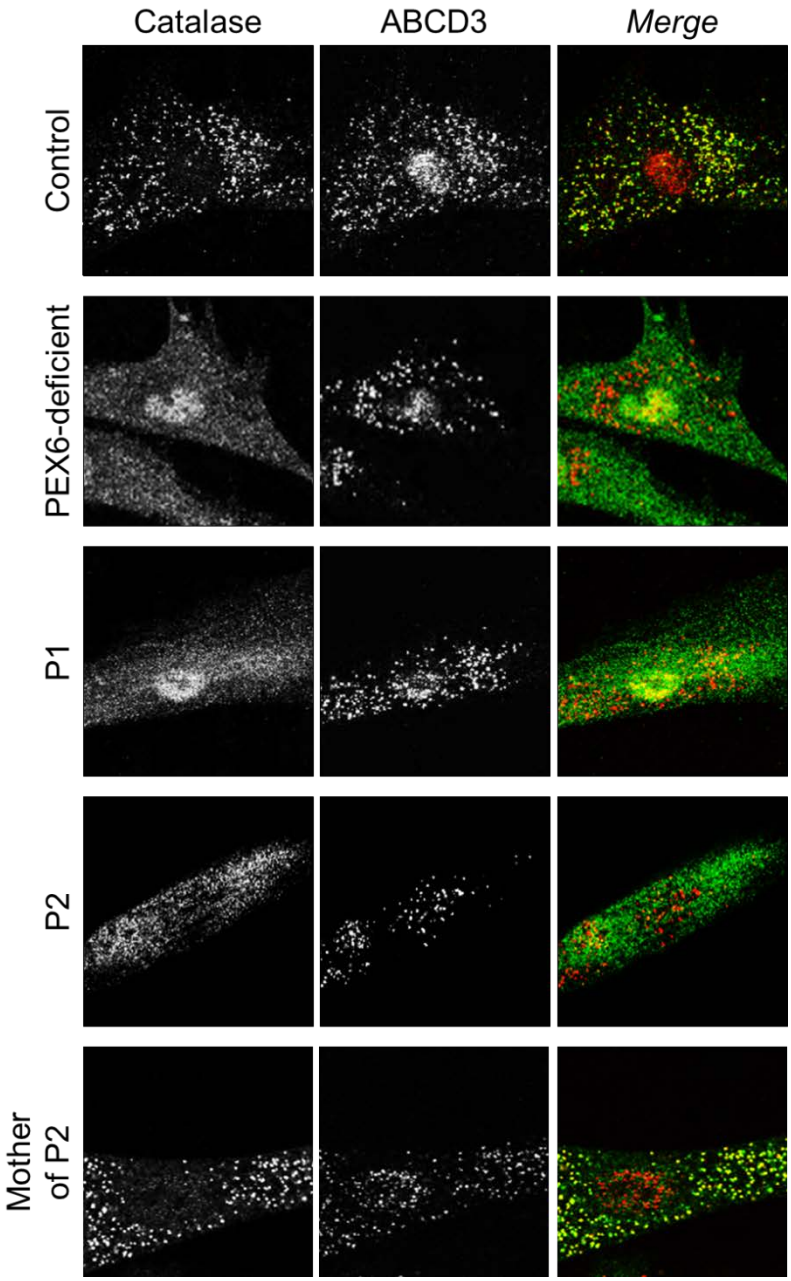

Figure S1 – Severe import defect of peroxisomal matrix protein catalase in affected individuals.

Immunofluorescence microscopy assay to determine the subcellular localization of the peroxisomal matrix protein catalase (green signal) and the peroxisomal membrane protein ABDC3 (red signal) in affected individuals. Catalase colocalized with ABCD3 to peroxisomes in control cells, but was mislocalized to the cytosol in PEX6-deficient cells. Also in fibroblasts derived from the affected individuals catalase was mislocalized to the cytosol indicating a severe catalase import defect. In contrast, catalase was only in few fibroblasts derived from the mother of individual P2 mislocalized, indicating a very mild catalase import defect.

A

PEX6	*H. sapiens*	842	V	F	V	I	G	A	T	N	R	P	D	L	L	D	P	A	L	L	R	P	G	R	F	D	K	L	V	F	V	870
PEX6	*M. musculus*	843	V	F	V	I	G	A	T	N	R	P	D	L	L	D	P	A	L	L	R	P	G	R	F	D	K	L	V	F	V	871
PEX6	*A. thaliana*	797	L	F	I	I	G	A	S	N	R	P	D	L	I	D	P	A	L	L	R	P	G	R	F	D	K	L	L	Y	V	825
PEX6	*D. melanogaster*	758	I	F	I	L	A	A	T	N	R	P	D	L	I	D	P	A	L	L	R	P	G	R	F	D	K	L	F	Y	V	786
PEX6	*S. cerevisiae*	871	V	F	V	I	G	A	T	N	R	P	D	L	L	D	E	A	L	L	R	P	G	R	F	D	K	L	L	Y	L	899
PEX6	*C. elegans*	866	V	I	I	L	G	C	T	S	R	I	D	L	I	D	D	A	L	L	R	P	G	R	F	D	H	H	V	Y	C	894
p97	*H. sapiens*	617	V	F	I	I	G	A	T	N	R	P	D	I	I	D	P	A	I	L	R	P	G	R	L	D	Q	L	I	Y	I	645
p97	*M. musculus*	617	V	F	I	I	G	A	T	N	R	P	D	I	I	D	P	A	I	L	R	P	G	R	L	D	Q	L	I	Y	I	645
NSF	*H. sapiens*	367	I	L	V	I	G	M	T	N	R	P	D	L	I	D	E	A	L	L	R	P	G	R	L	E	V	K	M	E	I	395
SRH consensus sequence			**V**	**-**	**V**	**I**	**-**	**A**	**T**	**N**	**R**	**P**	**D**	**-**	**L**	**D**	**P**	**A**	**L**	**L**	**R**	**P**	**G**	**R**	**-**	**D**	**R**	**-**	**I**	**-**	**-**	

B

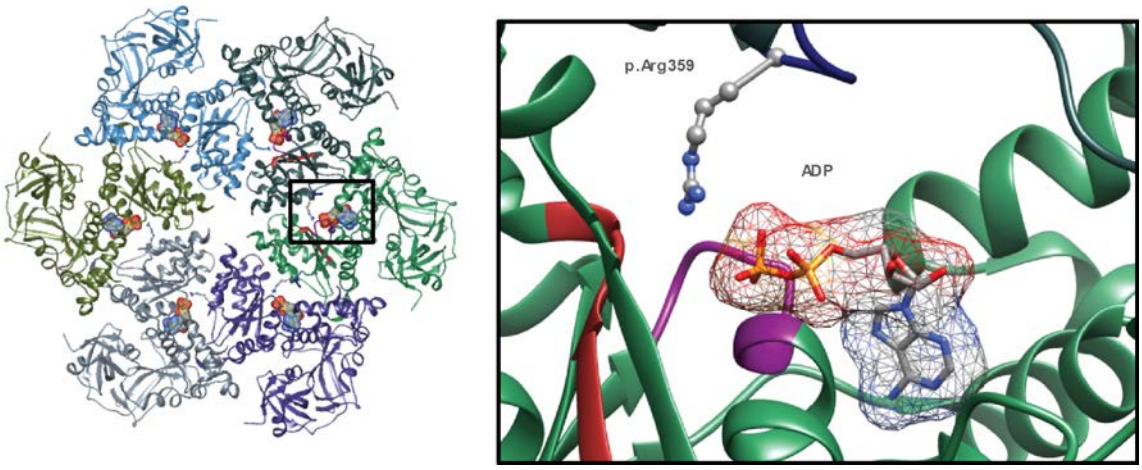

Figure S2 – Arginine finger 2 in the SRH of AAA+ ATPases.

(**A**) Multiple sequence alignment of protein sequences of various AAA+ ATPases, including PEX6 of different organisms, human and mouse p97 and human NSF [prepared based on alignments created by UniProt (www.uniprot.org)]. The alignment demonstrates the high conservation of arginine finger 2, which is mutated in the affected individuals and indicated in red. The SRH consensus sequence, which is described in [1], is indicated in grey. (**B**) 3D structure of an hexameric AAA+ ATPase complex, including the arginine finger 2 in the highly conserved SRH domain, which is located at the interface of two neighboring proteins in close vicinity to bound ADP (i.e. p.359Arg in the structure of p97of *M. musculus*, RCSB ID 1E32[2] , prepared using Chimera Software[3]).

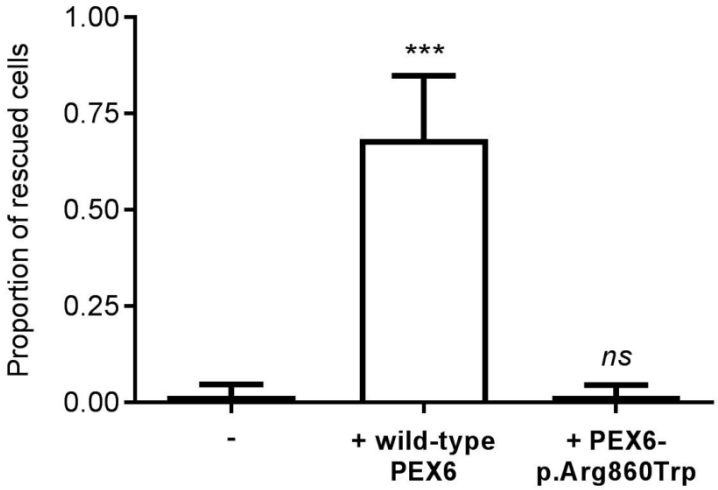

Figure S3 - The PEX6 variant p.Arg860Trp is pathogenic.

Functionality of PEX6-p.Arg860Trp variant. To determine whether PEX6-p.Arg860Trp can still support peroxisomal matrix import, we co-expressed the protein with a peroxisomal targeted GFP-SKL reporter in PEX6-deficient fibroblasts and determined the localization of GFP-SKL three days after transfection. Whereas co-expression of GFP-SKL with wild-type PEX6 results in restoration of peroxisomal matrix protein import in the majority of cells, we observed no complementation with PEX6-p.Arg860Trp, demonstrating that the mutant PEX6 protein is not functional. For this study, we determined the subcellular localization of GFP-SKL in 100-150 cells per condition in three to seven independent transfection experiments. Statistical analyses of the rescue efficiency of the co-transfected PEX6 variants versus non-transfected cells were performed using Mann-Whitney U test (*** $p \leq 0.001$, *ns* not significant).

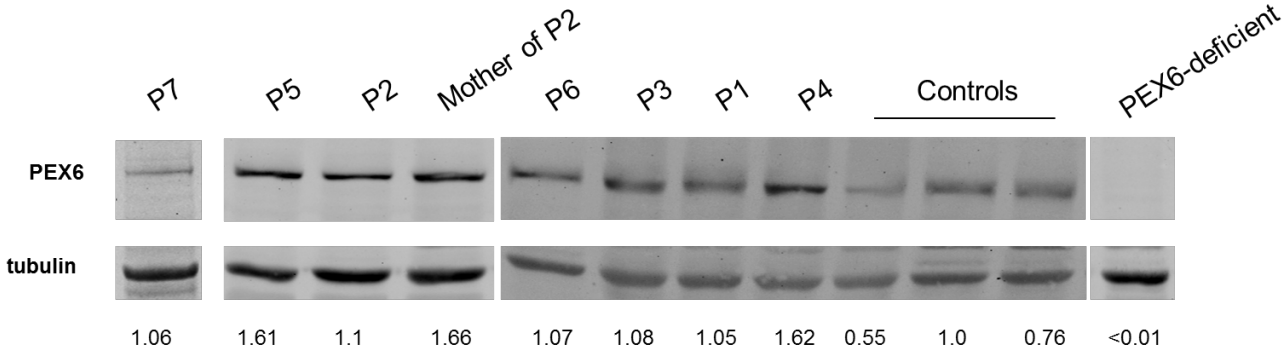

Figure S4 – PEX6 protein expression in affected individuals.

Immunoblot analyses on whole cell lysates of fibroblasts derived from the affected individuals, the mother of individual P2 or control individuals. Depicted are representative immunoblots using antibodies against PEX6 and against tubulin as a loading control which showed no marked changes in PEX6 protein expression in the affected individuals. To allow comparison of the PEX6 protein levels of samples run on different gels, we calculated the ratio PEX6:tubulin signal for each cell line and normalized these ratios per gel to the PEX6:tubulin ratio of the same control cell lysate run on each gel (set as 1.0).

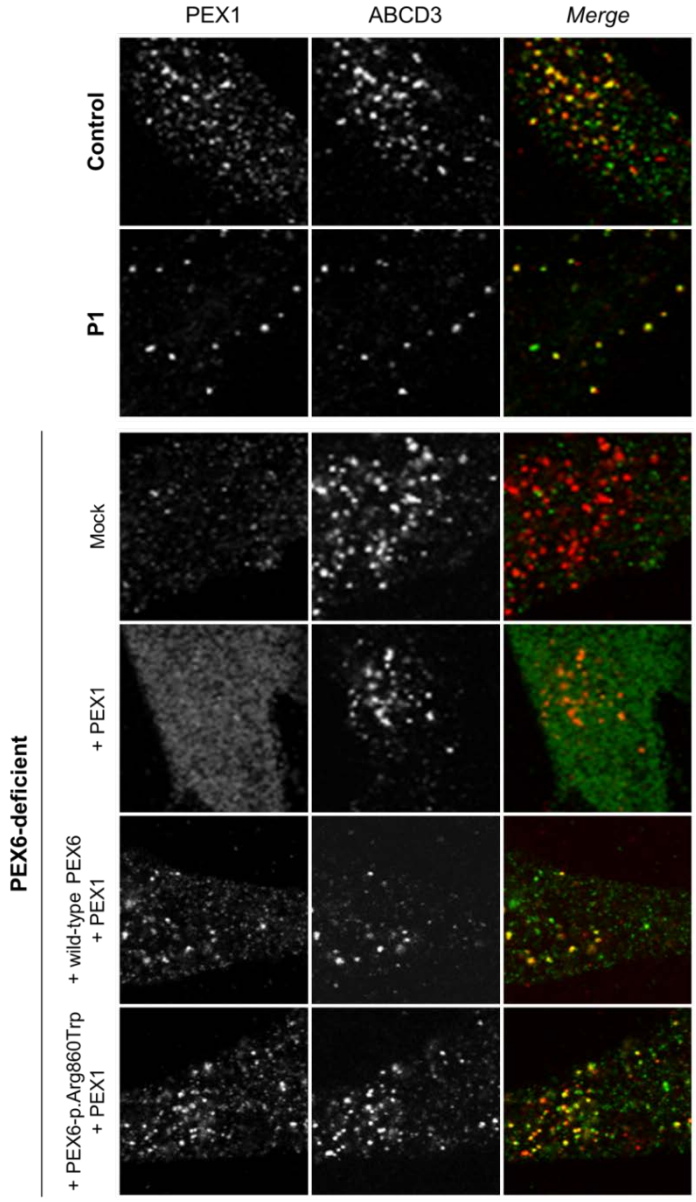

Figure S5 – PEX1/6 complexes are correctly localized to peroxisomes in cells of affected individuals and in PEX6-deficient cells expressing PEX6-p.Arg860Trp.

Immunofluorescence microscopy assay to determine the subcellular localization of PEX1 (green signal) and the peroxisomal membrane protein ACBD3 (red signal) in affected individuals. Because the localization of PEX1 to peroxisomes is strictly dependent on its interaction with PEX6, which in turn interacts with the peroxisomal membrane protein PEX26, a colocalization of PEX1 with ACBD3 indicates the peroxisomal localization of the PEX1-PEX6 complex. Both in cells of control individuals and cells of individual P1, PEX1 was localized to peroxisomes, indicating the correct localization of PEX1-PEX6 complexes in the cells of individual P1. In cells of a PEX6-deficient individual, endogenous and overexpressed PEX1 is not localized at peroxisomes ("Mock", "+ PEX1"). Transfection of the PEX6-deficient cells with either wild-type or PEX6-p.Arg860Trp and PEX1 confirmed that PEX6-p.Arg860Trp is indeed able to interact with PEX1 and localize the PEX1-PEX6 complex to the peroxisomes. Note that we used PEX1 antibodies for these studies, because PEX6 antibodies suitable for immunofluorescence microscopy were not available. The images represent a cellular area of 25x25µm.

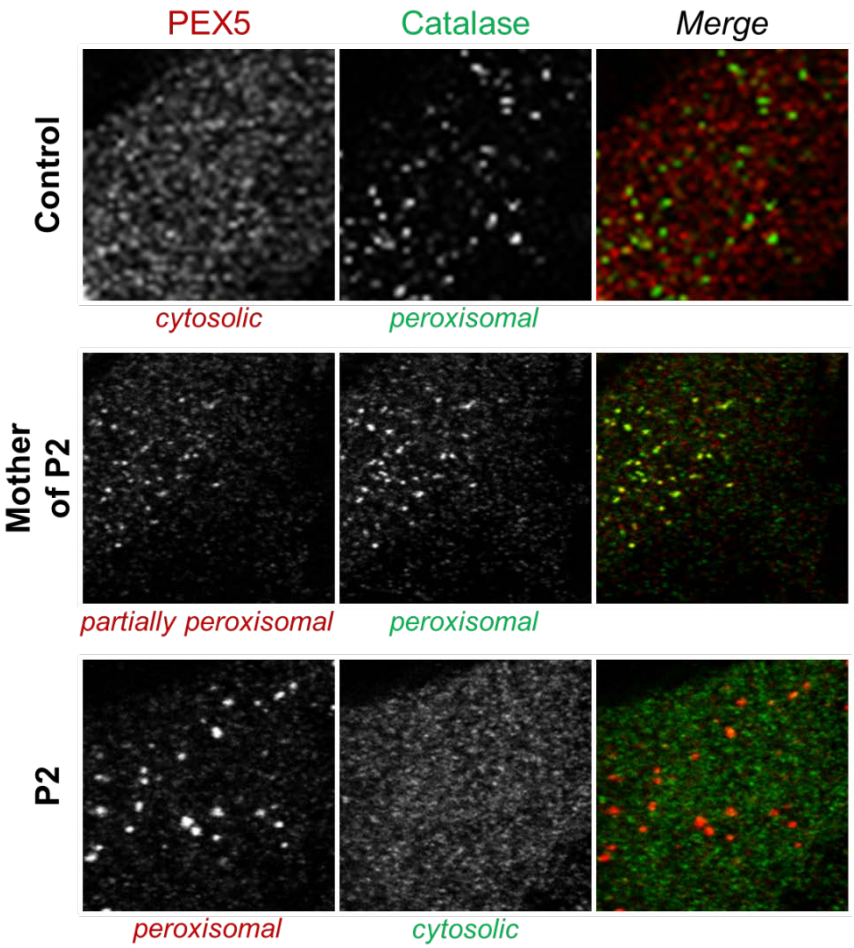

Figure S6 – PEX5 export defect in affected individuals.

Immunofluorescence microscopy assay to determine the subcellular localization of the peroxisomal matrix protein catalase (green signal) and the cytosolic protein receptor PEX5 (red signal) in affected individuals, including categories used in figure 1D. In control cells, catalase is localized in peroxisomes and PEX5 in the cytosol. In contrast, in cells of individual P2 catalase is mislocalized to the cytosol and PEX5 located at peroxisomes, indicative of the severe peroxisomal protein import defect. In cells of the mother of individual P2 PEX5 is partially peroxisomal. The images represent a cellular area of 25x25µm.

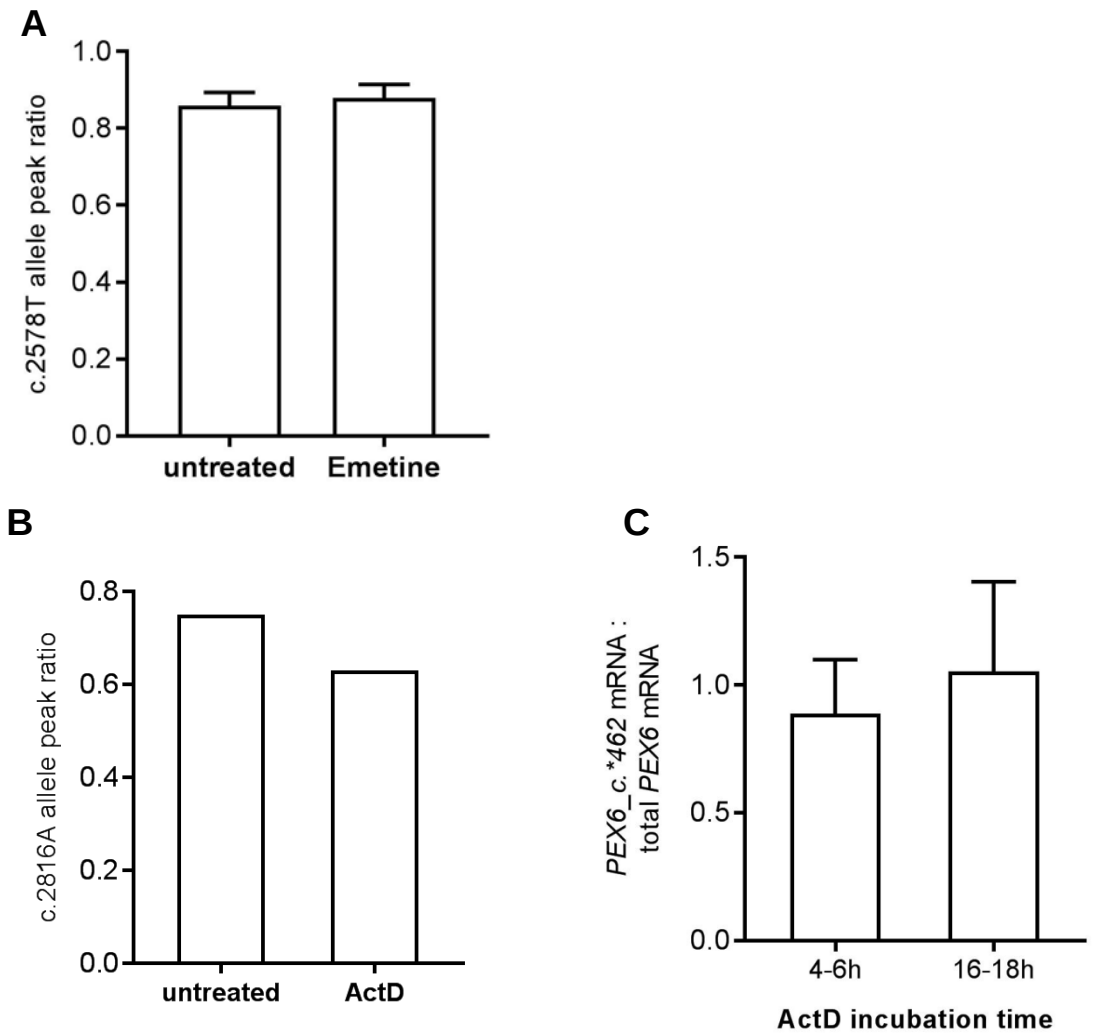

Figure S7 – Longer *PEX6-c.1_*462* mRNA is not less stable or more prone to nonsense-mediated mRNA decay (NMD)

Allelic expression of *PEX6* mRNA in cells treated with non-sense mediated mRNA decay-inhibitor emetine (A) or transcription inhibitor actinomycin D (B,C). **(A)** We treated fibroblasts of the affected individuals with the emetine, after which cDNA was prepared from RNA isolated from the cells. *PEX6* cDNA was Sanger sequenced and the allele peak ratio of the mutant *PEX6* allele c.2578T was determined as described in Figure 2B using in total 9 sequence reads from two independent experiments. The emetine-treated cells did not show an increase in the c.2578T peak ratio, which indicates that the long *PEX6-c.*1_462* mRNA encoded by the lower expressed allele (c.2578C) is not degraded by nonsense-mediated mRNA decay. **(B)** and **(C)** We treated fibroblasts derived from the affected individuals, as well as other cell lines heterozygous for the c.*442_445delTAAA variant and displaying AEI, with the actinomycin D (ActD, 1µM), after which cDNA was prepared from RNA isolated from the cells. **(B)** The cDNA was Sanger sequenced and the allele peak ratio of the common heterozygous polymorphism c.2816C>A was determined as described in Figure 2B using sequence reads from two independent experiments. Actinomycin D treated cells did not show an increase in the c.2816A ratio, which indicates that the long *PEX6-c.*1_462* encoded by the lower expressed allele (c.2816C) is not less stable. **(C)** We determined the ratio *PEX6-c.*1_462* mRNA : total *PEX6* mRNA using quantitative RT-PCR. We observed no decrease in the ratio, indicating that the longer *PEX6-c.*1_462* mRNA is not less stable than other *PEX6* mRNA. The ratio was normalized to the ratio of untreated cells in five independent experiments and is shown as mean with standard deviation.

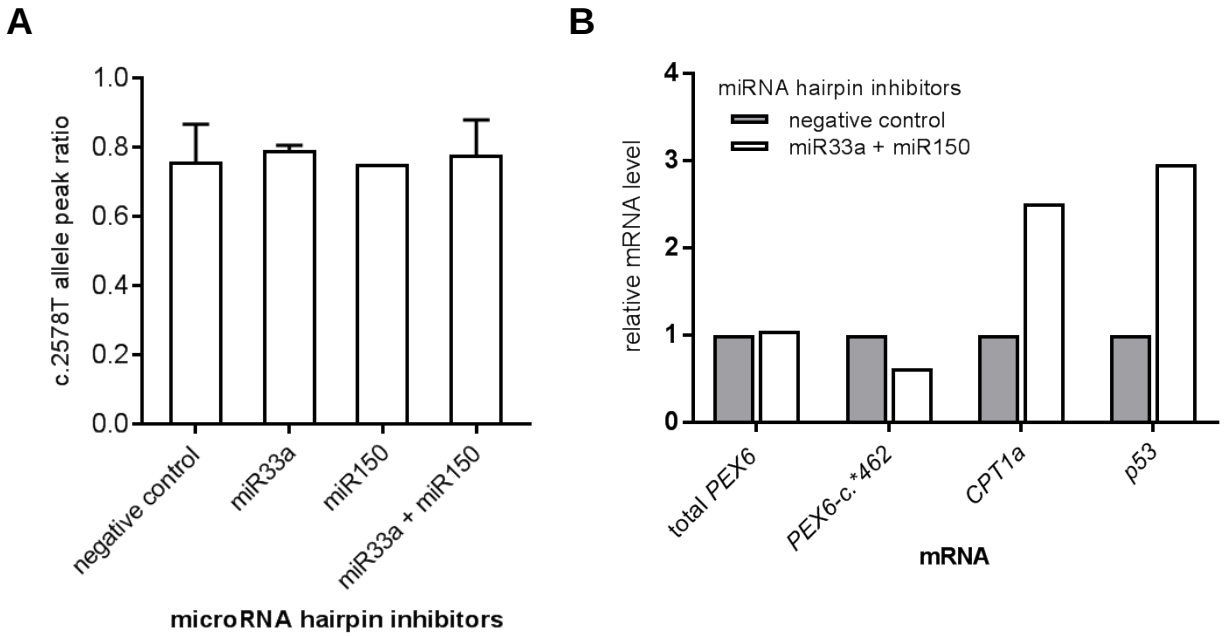

Figure S8 – Inhibitors of miRNAs hsa-miR-33a-5p and hsa-miR-150-5p do not affect AEI of *PEX6* in affected individuals.

Allelic *PEX6* mRNA expression in cells treated with miRNA inhibitors. We transfected fibroblasts derived from the affected individuals with negative control inhibitors or inhibitors of miRNAs predicted to target exclusively the long *PEX6-c.*1_462* for degradation (hsa-miR-33a-5p ("miR33"), hsa-miR-150-5p ("miR150")). (**A)** We analyzed whether the miRNA inhibition results in a decreased allele peak ratio of the variant c.2578C>T/C, as described in figure 2b. We observed no decrease of the ratio and thus no rescue of the AEI by miRNA inhibition, indicating that the decreased level of *PEX6-c.*1_462* is not mediated by miRNAs hsa-miR-33a-5p or hsa-miR-150-5p. Data are shown as mean with standard deviation of one to three independent experiments. (**B**) We analyzed whether the miRNA inhibition results in increased mRNA levels of *PEX6-c.*1_462.* Analysis of the mRNA levels using quantitative RT-PCR revealed no increase of *PEX6-c.*1_462* mRNA or total *PEX6* mRNA. The mRNA levels of the hsa-miR-33a-5p target gene *CPT1A* and the hsa-miR-150-5p target *p53* increased significantly, confirming the functionality of the miRNA inhibitors. mRNA levels were normalized to reference gene expression and the values of samples transfected with control mimics and are depicted as mean of two independent experiments.

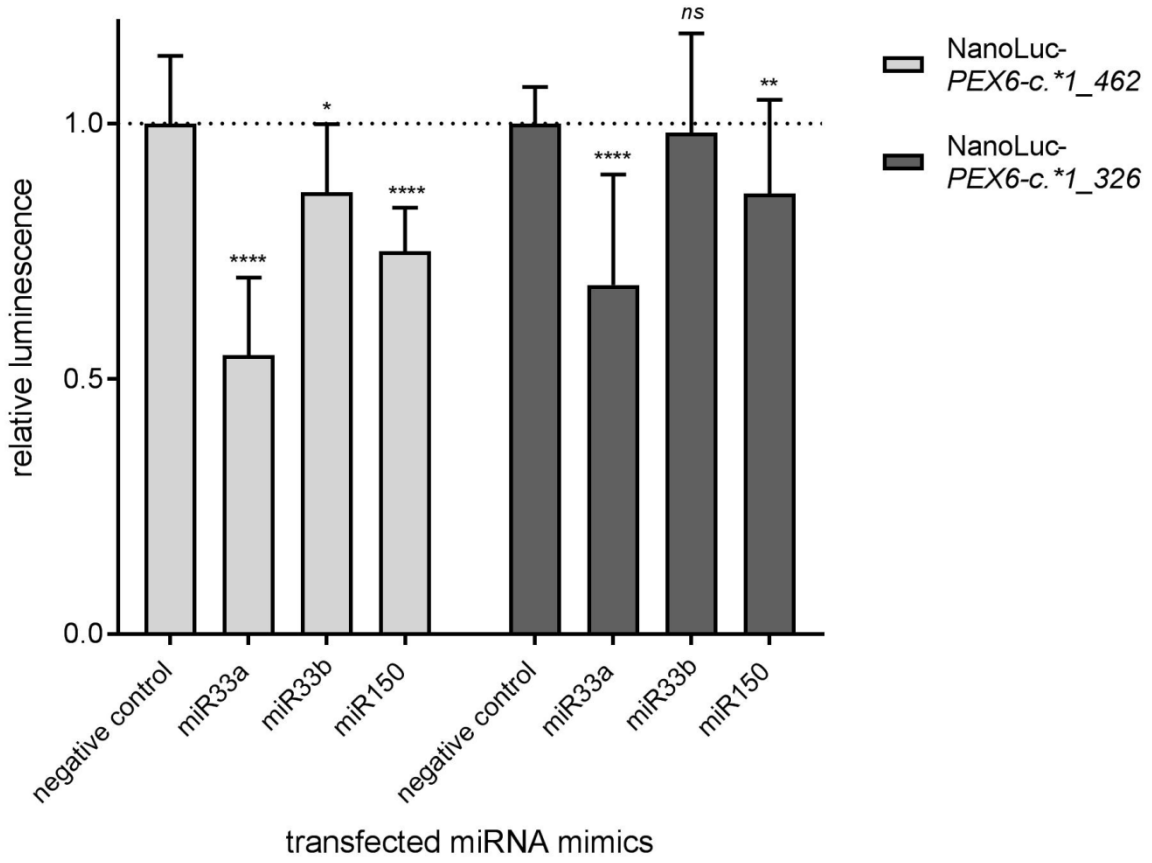

Figure S9 – miRNAs hsa-miR-33a-5p, hsa-miR-33b-5p or hsa-miR-150-5p do not specifically affect the signal of NanoLuc with the long *PEX6-c.*1_462* 3´-UTR..

Reporter gene assay of Nanoluc constructs with different PEX6-3'-UTRs treated with miRNA mimics. We transfected HEK293-FlpIn cells stably expressing NanoLuc constructs with the long *PEX6-c.*1_462* 3´-UTR (light grey) or the short *PEX6-c.*1_326* 3´-UTR (dark grey, used as control) with mimics of the indicated miRNAs and subsequently measured NanoLuc luminescence in three independent experiments. None of the miRNA mimics resulted in a stronger decrease of the luminescence signal of NanoLuc with the long *PEX6-c.*1_462* 3´-UTR when compared with the signal of NanoLuc with the short *PEX6-c.*1_326* 3´-UTR, indicating that the miRNAs do not cause a selective degradation of long *PEX6-c.*1_462* mRNA. The measured luminescence values were normalized to values of cells transfected with negative control mimics and are shown as mean with standard deviation. The statistical analyses were performed using Mann-Whitney U tests versus values of cells transfected with negative control mimics (* $p \leq 0.05$, ** $p \leq 0.01$, *** $p \leq 0.001$, **** $p \leq 0.0001$, *ns* not significant).

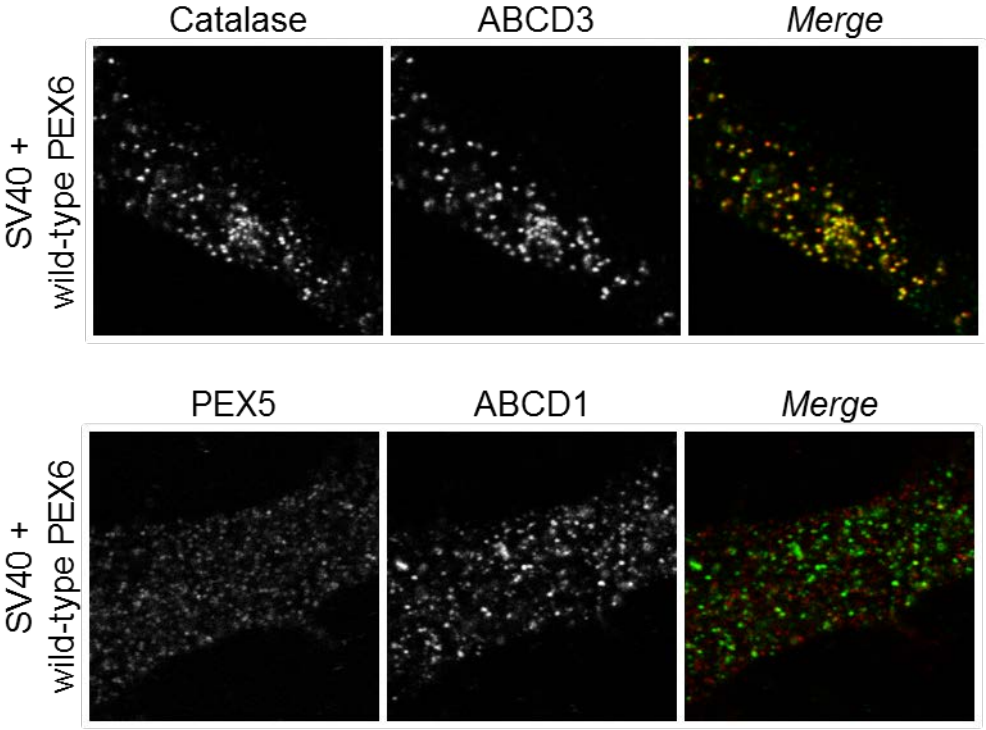

Figure S10 – SV40 immortalized control cells overexpressing wild-type PEX6 do not show a peroxisome biogenesis defect.

Immunofluorescence microscopy assay in SV 40 cells over expressing wild-type PEX6.We stably overexpressed PEX6-p.Arg860Trp or wild-type PEX6 in SV40 immortalized control fibroblasts and confirmed PEX6 overexpression by quantitative RT-PCR of isolated RNA and immunoblot analysis of PEX6 protein in cell lysates (data not shown). Subsequently, we used immunofluorescence microscopy to determine the subcellular localization of catalase and ABCD3, or PEX5 and ABCD1 in cells overexpressing PEX6-p.Arg860Trp (shown in Figure 3A) or wild-type PEX6 (shown here). The microscopic images of cells overexpressing wild-type PEX6 demonstrate that PEX6 overexpression does not result in a PEX5 export defect or a catalase import deficiency, in contrast to PEX6-p.Arg860Trp overexpression.

Table S1 – PEX6 primers.

PEX6_c.-1218fw	[-21M13]-CTGGGGCAGGAGATTCTTTG
PEX6_c.-619rev	[M13-Rev]-CAGCACATCTGGCACAAAACC
PEX6_c.-667fw	[-21M13]-TGAACAGGGCAAGAAGTCC
PEX6_c.50rev	[M13-Rev]-CGGTGTCTCGGTCGGAAAGG
PEX6_c.-860fw	[-21M13]-TTCCCCACCTTGTCATCTCCAG
PEX6_c.-744rev	[M13-Rev]-CCTTGCAGATCGGAAACCCA
PEX6_c.-844rev	[M13-Rev]-AACAGTCGACTTCCTGCGTG
PEX6in0 forw	[-21M13]-TGACGGAAGCGGAAGCGGCCCTCG
PEX6ex1arevII	[M13-Rev]-AAACCGCAAAGGAGGACACC
PEX6e1b forw	[-21M13]-TAGGTTGGGCACTGCTTGG
PEX6IN1 revII	[M13-Rev]-TATGTTCAAAGTCCGGGATG
PEX6exon2 forw	[-21M13]-TGCTGAGAGACAGGTTAGAG
PEX6exon2 rev	[M13-Rev]-ATTACAGACGTGAGCCACAG
PEX6ex3-fw	[-21M13]-TTGTTCCTTGGAGAACTGCG
PEX6ex3-rev	[M13-Rev]-ACTCATGCACCCAGGTTAC
PEX6e4/5 forw	[-21M13]-TGTTTGTCCTCTGTGATTGAG
PEX6e4/5 rev	[M13-Rev]-ACTCTGGCCAGTTCATTAGG
PEX6e6/7 forw	[-21M13]-TCTAAGGGATCTTGTGTTACTG
PEX6ex7-rev	[M13-Rev]-CCCCCAGCTTTGAGAGGC
PEX6ex8-fw	[-21M13]-ACAAGGCAGTCCACAGGAG
PEX6ex8-rev	[M13-Rev]-TATAACAAAAGCCAGGGACC
PEX6ex9-fw	[-21M13]-TGCCCTGCTCATGTGTCCT
PEX6ex9-rev	[M13-Rev]-TTCCGCCTTTCTGGTGCC
PEX6e10/11 forw	[-21M13]-ATGGGACGCTGATGGTGAG
PEX6e10/11rev	[M13-Rev]-GAGCCGTCAGATGCACATAC
PEX6e12/13forw	[-21M13]-GTATGTGCATCTGACGGCTC
PEX6e12/13rev	[M13-Rev]-TCTCTGGACTCTGAAGACTG
PEX6e14/15forw	[-21M13]-TAAAGAGAGGTACCACAGGC
PEX6e14/15rev	[M13-Rev]-TGTTGCATGCATCCCCTAAG
PEX6e16/17 forw	[-21M13]-TGCATGCAACATGCAGGATG
PEX6e16/17 rev	[M13-Rev]-TCTCTCTGTGGGCTATCAAG
PEX6_c.2807-21fw	[-21M13]-TCCCCACCTTGTCATCTCCAG
PEX6_c*541rev	[M13-Rev]-GCCTCTAGAGCAGACTACAGC
PEX6_c.625fw	[-21M13]-TCCTCGTTGGTGTCCTGTC
PEX6_c.-22rev	[M13-Rev]-GTGCCAGAAACCGCAAAGG
PEX6_c.491fw	[-21M13]-CCAGACTGTGTCCAGAGTC
PEX6_c.1075rev	[M13-Rev]-CACATAGAACATCCCCTTCC
PEX6_c.951fw	[-21M13]-TGCCAGAGAGTTACACATCG
PEX6_c.1541rev	[M13-Rev]-ATGGCCTGCAGTTTTGTCTC
PEX6_c.1422fw	[-21M13]-TGGGAAGACCACAGTAGTTG
PEX6_c.1988rev	[M13-Rev]-TCCTCCTCAGTCAAGCCAC
PEX6_c.1856fw	[-21M13]-ACTTGGCACAGCTAGCACG
PEX6_c.2468rev	[M13-Rev]-TCCATCACTCCTCCAGAATC
PEX6_c.2339fw	[-21M13]-AAAGTGAGGAGAATGTGCGG
PEX6_c.3004rev	[M13-Rev]-TCTGTGGGCTATCAAGGTAC
Pex6_2330fw	ATGTGGGCCAAAGTGAGGAG

Pex6_c.2282fw	GTGCAGCCTTACCTTCCTCAG
PEX6attB2-rev	GGGGACCACTTTGTACAAGAAAGCTGGG TCCTAGCAGGCAGCAAACTTGC
PEX6-3end_mRNA_c2761fw	[-21M13]-GCTATGACAGCTGCCCTCAA
PEX6-3end_mRNA_c*459rev	[M13-Rev]-GCATGCATTGTGTTTATTTATGTCA
qPCR_PEX6_c.2466fw	GGACAGGGTGGTGTCTCAG
qPCR_PEX6_c.2566rev	GGTCCAGGAGATCTGGTCTG
qPCR_PEX6_c.*231fw	CATCTACTCAGGAAGAGGGCC
qPCR_PEX6_c.*375rev	CCACAACCCTGCTCTTTCTC

[M13-Rev], CAGGAAACAGCTATGACC; [-21M13], GTAAAACGACGGCCAGT

Table S2 – Peroxisomal parameters in blood of affected individuals & family members.

	individual	**P2**	**Half-brother of P2**	**Mother of P2**	**P3**	**P4**	**Father of P4**	**P5**	**P6**	**P7**
	age at sampling	8 mo	9 yo	21 yo	*n/a*	7 yo	*n/a*	*n/a*	*n/a*	1 yo
VLCFA concentration	C22:0	0.457% (1.18 ± 0.61)	0.292% (1.18 ± 0.61)	1.002% (1.18 ± 0.61)	33.1µmol/l (55.1-11.43)	58µmol/l (28-76)	46µmol/l (16-76)	*n/a*	0.610% (1.18 ± 0.61)	18.62 µmol/l (40.3-103.7)
	C24:0	0.723% (0.78 ± 0.32)	0.668% (0.78 ± 0.32)	0.764% (0.78 ± 0.32)	47.9µmol/l (44.3-92.4)	65µmol/l (22-63)	40µmol/l (15-61)	*n/a*	0.818% (0.78 ± 0.32)	33.27 µmol/l (32.3-93.7)
	C25:0	0.076% (0.03 ± 0.03)	0.058% (0.03 ± 0.03)	0.026% (0.03 ± 0.03)	*n/a*	1.8µmol/l (0-2)	1.1µmol/l (1-1.3)	*n/a*	0.061% (0.03 ± 0.03)	*n/a*
	C26:0	0.093% (0.01 ± 0.01)	0.144% (0.01 ± 0.01)	0.008% (0.01 ± 0.01)	5.2µmol/l (0.220-0.880)	2.6µmol/l (0-0.8)	1.2µmol/l (0-0.74)	*n/a*	0.066% (0.01 ± 0.01)	6.29 µmol/l (0.35-1.36)
		2.171µg/ml (0.33 ± 0.18)	1.937µg/ml (0.33 ± 0.18)	0.22µg/ml (0.33 ± 0.18)	*n/a*	*n/a*	*n/a*	*n/a*	1.42µg/ml (0.33 ± 0.18)	*n/a*
	C26:1	*n/a*	0.432µg/ml (0.29 ± 0.19)	0.44µg/ml (0.29 ± 0.19)	*n/a*	*n/a*	*n/a*	*n/a*	0.42µg/ml (0.29 ± 0.19)	*n/a*
VLCFA ratios	C24:0/C22:0	1.573 (0.84 ± 0.08)	2.287 (0.84 ± 0.08)	0.762 (0.84 ± 0.08)	1.40 (0.55-0.89)	1.11 (0-1.1)	0.96 (0-1.09)	1.225 (0.55-1.115)	1.341 (0.33 ± 0.18)	1.79 (0.69-1.08)
	C26:0/C22:0	0.204 (0.01 ± 0.01)	0.492 (0.01 ± 0.01)	0.008 (0.01 ± 0.01)	0.157 (0.004-0.021)	0.045 (0-0.02)	0.028 (0-0.019)	0.194 (0- 0.035)	0.108 (0.01 ± 0.01)	0.338 (0.006-0.019)
Phytanic acid		*n/a*	0.105 µg/ml (0-3)	*n/a*	2.8µg/ml (0-2.0)	5.2 µmol/l (0-5)	29.5µmol/l (0-5.9)	12 mg/100ml (0- 0.7)	10.5 µg/ml (0-3)	26.94 µmol/l (1.44-10.98)
Pristanic acid		*n/a*	*n/a*	*n/a*	1.7µg/ml (0-1.0)	2.5 µmol/l (0-1)	16.6µmol/l (0-1.2)	*n/a*	*n/a*	10.32 µmol/l (0.06-1.42)
Pipecolic acid		*n/a*	2.9 µmol/l (0.7-2.6)	*n/a*	*n/a*	*n/a*	*n/a*	*n/a*	8.8 µmol/l (0.7-2.6)	82 µmol/l (0-6)

VLCFA, very long-chain fatty acids; mo, months old; yo, years old; *n/a,* not assessed; numbers between brackets indicate the reference range according to the laboratory in which the assays have been performed. Values measured in asymptomatic parents are depicted with a light grey background.

Supplemental references

1. Karata K, Inagawa T, Wilkinson AJ, Tatsuta T, Ogura T. Dissecting the role of a conserved motif (the second region of homology) in the AAA family of ATPases. Site-directed mutagenesis of the ATP-dependent protease FtsH. J Biol Chem 1999;274(37):26225–32.
2. Zhang X, Shaw A, Bates PA, et al. Structure of the AAA ATPase p97. 2000;6:1473–84.
3. Pettersen EF, Goddard TD, Huang CC, et al. UCSF Chimera - A visualization system for exploratory research and analysis. J Comput Chem 2004;25(13):1605–12.